Published in final edited form as:
Innate Immun. 2012 December ; 18(6): 825–833. doi:10.1177/1753425912442431.

Hepatic uptake and deacylation of the lipopolysaccharide in bloodborne lipopolysaccharide-lipoprotein complexes

Baomei Shao[1], **Robert Munford**[1,2], **Richard L. Kitchens**[1], and **Alan W. Varley**[1,*]

[1]Department of Internal Medicine, Division of Infectious Diseases, The University of Texas Southwestern Medical Center, Dallas, Texas [2]Laboratory of Clinical Infectious Diseases, National Institute of Allergy and Infectious Diseases, National Institutes of Health, Bethesda, Maryland

Abstract

Much evidence indicates that bacterial lipopolysaccharide (LPS, endotoxin) is removed from the bloodstream mainly by the liver, yet the hepatic uptake mechanisms remain uncertain and controversial. In plasma, LPS can be either “free” (as aggregates, bacterial membrane fragments, or loosely bound to albumin, CD14, or other proteins) or “bound” (complexed with lipoproteins). Whereas most free LPS is taken up by Kupffer cells, lipoprotein-bound LPS has seemed to be cleared principally by hepatocytes. Here we compared the liver’s ability to take up and deacylate free LPS aggregates and the LPS in preformed LPS-HDL (high density lipoprotein) complexes. In mice examined from 1 hour to 7 days after a small amount of fluorescent (FITC-)LPS was injected into a lateral tail vein, we found FITC-LPS almost entirely within, or adjacent to, Kupffer cells. As expected, FITC-LPS complexed with HDL (FITC-LPS-HDL) disappeared more slowly from the circulation and a smaller fraction of the injected dose of FITC-LPS was found in the liver. Unexpectedly, the FITC-LPS injected as FITC-LPS-HDL complexes was also found within sinusoids, adjacent to or within Kupffer cells. In other experiments, we found that both free and HDL-bound radiolabeled LPS underwent enzymatic deacylation by acyloxyacyl hydrolase (AOAH), the LPS-inactivating enzyme that is principally produced within the liver by Kupffer cells. Our observations suggest that Kupffer cells and AOAH play important roles in clearing and catabolizing both free LPS and the LPS in circulating LPS-HDL complexes.

Keywords

LPS; acyloxyacyl hydrolase; HDL; endotoxin; deacylation; clodronate; Kupffer cell; liposome

INTRODUCTION

The intrasinusoidal hepatic macrophages known as Kupffer cells are often credited with removing Gram-negative bacterial LPS from the circulating blood. This conclusion has been

*Address correspondence to Alan W. Varley, Department of Internal Medicine, Division of Infectious Diseases, UT Southwestern Medical Center, 5323 Harry Hines Blvd, Dallas, Texas, 75390-9113, Tel. 214-648-8093; Fax. 214-648-9478; alan.varley@UTSouthwestern.edu.
[2]Current address for RSM is the Laboratory of Clinical Infectious Diseases, National Institute of Allergy and Infectious Diseases, National Institutes of Health, Bethesda, Maryland 20815

reached by many of the investigators who have injected LPS intravenously into animals and studied its uptake by the liver. The methods used to identify the hepatic cells that take up bloodborne LPS have included autoradiography (1;2), immunostaining using anti-LPS antibodies (3–5), tracking fluorescent LPS molecules using confocal microscopy (6;7), and detection of LPS bioactivity using horseshoe crab amoebocyte factor C (8–10). Other investigators have injected radiolabeled LPS intravenously, isolated individual hepatic cell types, and quantitated LPS uptake using scintillation counting (5;11). In each of these studies, LPS was detected most abundantly, and sometimes almost exclusively, in Kupffer cells. In some, neutrophils were found to take up the LPS and then undergo phagocytosis by Kupffer cells (12).

On the other hand, there is also evidence that LPS can be taken up by both sinusoidal endothelial cells (SEC) and hepatocytes. Some of these studies used isolated SECs or hepatocytes that were exposed ex vivo to LPS; others found LPS associated with these cell types *in vivo* following intravenous LPS injection (3;9;10;13–15). In addition, LPS exposure can enhance the uptake of latex beads by SEC *in situ*, raising the possibility that these cells, if activated, might also take up LPS *in vivo* (16). In one indirect approach, FITC-LPS was injected intravenously and recovered from the bile within a few minutes (17); rapid transit through hepatocytes was suggested. In another, studies of the kinetics of ^{3}H-LPS binding in buffer-perfused livers found that depleting Kupffer cells with gadolinium allowed hepatocytes to clear LPS effectively from the perfusate (18).

These studies have not addressed the role that the physical state of bloodborne LPS might play in determining its fate in the liver. In plasma, LPS can be either “free” (as aggregates, bacterial membrane fragments, or loosely bound to albumin, soluble CD14, or other proteins) or complexed with lipoproteins. Binding to high density lipoprotein (HDL), LDL, VLDL or chylomicrons occurs within seconds when LPS is incubated *in vitro* with serum or plasma (19). A major determinant of binding is the phospholipid content of the lipoprotein particles, which correlates with their surface area (20). Mediated largely by LPS binding protein (LBP)(21;22), lipoprotein binding also occurs quickly *in vivo*; it has been generally thought to target the LPS to cells, such as hepatocytes, that can take up the lipoprotein(s) via specific receptors (23–25). Lipoprotein-bound LPS is cleared more slowly from the bloodstream and is less able to stimulate cells than is free LPS, presumably because its lipid A moiety is sequestered within the lipoprotein micelle (26–28).

Important mechanisms modulate hepatic responses to LPS. A critical catabolic step requires the enzyme acyloxyacyl hydrolase (AOAH), which inactivates LPS by removing the secondary fatty acyl chains from its lipid A moiety (29). AOAH is expressed by various phagocytes, including Kupffer cells (KC) and hepatic dendritic cells (6). Studies performed in AOAH-deficient mice revealed that even small doses of bioactive LPS can persist in cells and tissues for weeks, resulting in chronic cell activation and prolonged macrophage tolerance to LPS and other microbial stimuli; the presence of fully acylated LPS is accompanied by immunosuppression and long-lasting pathologies such as hepatomegaly and exaggerated polyclonal antibody responses (6;7;30;31). Although LPS may also be inactivated *in vivo* by intravenous injections of alkaline phosphatase (32;33) and there is

evidence that intestinal alkaline phosphatase may inactivate LPS in the gut (34;35), endogenous tissue phosphatases are unable to inactivate LPS in mice that lack AOAH.

Here we compared the intrahepatic fates of LPS and LPS-HDL complexes. We found that free LPS is taken up initially by Kupffer cells and that some of this LPS remains KC-associated for at least 7 days. Although the LPS in LPS-HDL complexes was taken up by the liver more slowly than was free LPS, it gradually became associated with KCs and underwent enzymatic deacylation within the liver. The findings show that KCs and AOAH play important roles in deacylating both free and HDL-bound LPS.

METHODS

LPS preparation, labeling

We prepared fluorescent LPS (FITC-LPS) by suspending 2.4 mg of pure *E. coli* O14 LPS (Ra chemotype), prepared using the phenol-chloroform-petroleum ether method of Galanos (36), in 1.2 ml 0.1M Na borate (pH 10.5). After water bath sonication until the suspension was translucent, we added 10 mg FITC (Invitrogen) and incubated the mixture for 3 hr at 37°C. Glycine (10.75 mg) was added to stop the reaction and the mixture was dialyzed (1000 MW cutoff) against PBS at 4°C, with daily changes until no yellow color appeared in the PBS. The FITC-LPS was precipitated by adding 2 volumes of 100% ethanol and the pellet was washed 3 times with 70% ethanol before being suspended in pyrogen-free water (1.2 mg/ml). Approximately 50% of the LPS was recovered; the FITC/LPS molar ratio in the conjugate was 0.53. The activity of FITC-LPS was tested by incubating different amounts of FITC-LPS or LPS with peritoneal macrophages for 6 hrs *in vitro* and measuring IL-6 in the culture medium; the two dose-response curves were superimposable (not shown). FITC sodium salt and FITC-BSA were from Sigma. Each of the preparations was suspended in sterile, endotoxin-free PBS prior to injection.

Biosynthetically labeled *Salmonella typhimurium* PR122 (Rc structure) [^{3}H/^{14}C]LPS (1.2×10^{5} dpm ^{3}H/μg LPS in the fatty acyl chains and 8×10^{3} dpm ^{14}C/μg LPS in the lipid A glucosamine backbone) was used to measure LPS clearance, uptake, and deacylation (8). To prepare LPS-HDL complexes, we incubated 100 μg [^{3}H/^{14}C]LPS and 100 μg FITC-LPS with 10 mg human HDL (provided by Y.K. Ho, UT Southwestern Medical Center) and 2 μg recombinant human LPS-binding protein (37) for 6 hrs at 37°C, 150 mM NaCl, 100 mM HEPES, pH 7.4. The density of the solution was adjusted to 1.21 g/ml with KBr and the FITC-LPS-HDL complexes were isolated by ultracentrifugal flotation (38). After dialysis against 0.9% NaCl, 3 mM EDTA at 4°C, the FITC-LPS-HDL and uncomplexed HDL were filtered (0.45 μm, Amicon) and stored at 4°C. Approximately 60% of the radiolabeled LPS floated at the top of the gradient (the position occupied by HDL), whereas less than 3% was found at the top of the gradient in the absence of HDL (control). As expected (26), the ability of the LPS to induce macrophage IL-6 production in vitro was reduced 10-fold in LPS-HDL complexes (not shown).

Mouse strains

Wildtype and *Aoah*$^{-/-}$ C57BL/6 mice (39) were maintained in specific pathogen-free conditions in the UT Southwestern Animal Resources Center and used for experiments when they were 5 – 12 weeks of age. On one occasion, serology for murine norovirus was positive for sentinel mice. All protocols were approved by the UT Southwestern Institutional Animal Care and Use Committee.

LPS administration and specimen preparation

Mice were injected with FITC-LPS or [^{3}H/^{14}C]LPS (5–10 μg/mouse), FITC-LPS plus [^{3}H/^{14}C]LPS (total of 10 μg per mouse, mixed prior to injection), LPS-HDL complexes (FITC-LPS-HDL plus [^{3}H/^{14}C]LPS-HDL (total of 10 μg LPS)), FITC sodium salt (0.6 μg/mouse), or FITC-BSA (10 μg BSA/mouse). Injections were given into the lateral tail vein in a volume of 200 μl. At sequential time points (1 hr, 4 hrs, 24 hrs, and 3 and 7 days) after injection, the livers, spleens, kidneys, and (in some experiments) abdominal fat were harvested. Small liver pieces were embedded in OCT compound and frozen in liquid nitrogen; other pieces of liver, spleen, kidney and fat were lysed by sonication in lysis buffer (PBS with 0.2% Triton X-100, 5 mM EDTA) and aliquots were subjected to scintillation counting as previously described (8). In other experiments, *Aoah*$^{-/-}$ mice were given i.v. injections containing clodronate-liposomes or PBS-liposomes (prepared in the laboratory of Jerry Niederkorn, UT-Southwestern, from clodronate provided by Roche, or in the laboratory of R. Munford at NIAID, using clodronate purchased from Sigma-Aldrich). Forty-eight hrs after liposome treatment, half of the clodronate- or PBS-liposome-treated mice were injected with 10 μg FITC-LPS or PBS mixed with 2 μg [^{3}H/^{14}C]LPS. The livers from each group were harvested four hours, 1 day or 6 days after the LPS injection.

LPS uptake and deacylation

The [^{3}H/^{14}C]LPS contains a ^{14}C-glucosamine-labeled lipid A backbone and ^{3}H-labeled fatty acyl chains. The ^{14}C content reflects the number of LPS molecules in the sample and the ratio of ^{3}H to ^{14}C dpm is determined by the number of fatty acyl chains per LPS molecule. Because the ^{14}C radioactivity remaining in the plasma following i.v. LPS injection was very low at some time points, we used the ^{3}H dpm to follow LPS disappearance from the blood over time. Measurements of LPS deacylation were performed as previously described (*Method 2* in (6)). Briefly, the ^{14}C-labled LPS with its remaining ^{3}H-labeled fatty acyl chains was precipitated from tissue lysates by adding 2 volumes of ethanol, leaving the released ^{3}H-fatty acids, lipid metabolites, and any ethanol-soluble degradation products in the supernatant. Deacylation was calculated by comparing the ^{3}H /^{14}C ratio of the ethanolinsoluble material to that of the initial ^{3}H /^{14}C ratio of the LPS: % deacylation = 1 – [measured ^{3}H /^{14}C ratio]/[starting ^{3}H /^{14}C ratio]) x 100. Since 2 of the 6 fatty acyl chains are secondary chains that can be removed by AOAH, the percent removal of secondary acyl chains was calculated by the formula: % deacylation of secondary chains = % deacylation/0.33.

Microscopy

Six μm cryostat liver sections were fixed with cold 70% methanol/30% acetone for 15 min at −20°C. After blocking with normal mouse IgG and BSA, they were stained with rat anti-mouse CD144 antibody (11D4.1; BD Pharmingen) followed by Alexa Fluor® 555-conjugated goat anti-rat IgG (Invitrogen) to identify endothelial cells, or with biotin-conjugated rat anti-mouse CD11b antibody (M1/70; BD Biosciences Pharmingen) followed by Alexa Fluor® 555 conjugated streptavidin (Invitrogen) to identify neutrophils. Alexa Fluor® 647-conjugated rat anti-mouse F4/80 antibody (BM8; Invitrogen) was added to identify Kupffer cells and Qdot® 565-conjugated goat anti-FITC antibody (Invitrogen) was added to amplify the FITC signal. Nuclei were stained with DAPI. Images were taken using a Leica TCS SP5 confocal microscope in the Live Imaging Core (UT Southwestern, Kate Luby-Phelps, Director). Livers from three mice per group were studied by immunofluorescence microscopy at each time point. Multiple (at least 3) images were taken at 63X magnification from each section. One selected field from each of these images was recorded at a higher magnification using a 2.4X zoom. Semi-quantitative analysis of higher magnification (63X with 2.4X zoom) images was performed in a blinded fashion on coded images by overlaying three single color images (CD144, F4/80, and LPS) in Adobe Photoshop to determine whether FITC-LPS areas overlapped with or were directly adjacent to CD144+ or F4/80+ areas of the liver section. The intensity of the bright (+++) areas of FITC-LPS were assumed to reflect at least one log (10-fold) more LPS than was present in the dim areas. Therefore, dim (+), medium (++), and bright (+++) areas of FITC-LPS were assigned the numbers 1, 3, and 10, respectively, to approximate the relative amounts of LPS on a logarithmic scale. The amount of LPS associated with CD144 and/or F4/80 was determined as the percentage of the total numerical sum of LPS intensities in each group. Statistical analysis was based on percentages derived from each image (usually n=6 images from 3 mice/group).

KC depletion and LPS deacylation

AOAH-wildtype mice were injected i.v. with 200 μl clodronate-liposomes or PBS-liposomes. Two days later, the mice were injected i.v. with 5 μg of [^{3}H/^{14}C]LPS or HDL-[^{3}H/^{14}C]LPS. The spleen and liver were harvested four hours after LPS injection. A small piece of liver (around 180mg) and the spleen were lysed by sonication in lysis buffer (PBS with 0.2% Triton X-100, 5 mM EDTA). Tissue LPS uptake and deacylation were calculated as described above, and sections of liver and spleen were examined for the presence of Kupffer cells as described above. Clodronate-liposomes reproducibly depleted 90% of the F4/80-positive cells.

Statistics—We tested for significant differences between groups using the two-tailed Student's "t" test.

RESULTS

Uptake of radiolabeled LPS and LPS-HDL complexes by the liver

Within one hour of injecting [^{3}H/^{14}C]LPS into the tail vein, over 90% of the LPS had been cleared from the circulation and approximately 90% of the injected ^{14}C dpm (a marker for

the carbohydrate backbone of LPS) was found in the liver (Figure 1A, B). The [^{3}H/^{14}C]LPS in LPS-HDL complexes was cleared much more slowly (about 50% was still in plasma at this time point), and only 15% of the injected ^{14}C dpm had accumulated in the liver. In contrast, the uptake of [^{3}H/^{14}C]LPS-HDL by the kidney and abdominal fat exceeded that of [^{3}H/^{14}C]LPS (Figure 1C). The slower clearance rate and tissue distribution confirm previous findings (3,10,11) and provide additional evidence that the LPS-HDL complexes were formed as expected.

Intrahepatic locations of LPS and LPS-HDL

VE-cadherin is an important constituent of endothelial cell junctions. Its location can provide an approximate outline of the hepatic sinusoids (red in Fig. 2A, white in Fig. 2 C–E). An antibody to F4/80 was used to identify KCs (red, Fig. 2B–E). DAPI (blue) stains cell nuclei. Qdot®565 nanocrystal (conjugated to an anti-fluorescein antibody) were used to amplify the FITC signal (green). Using these markers, it was possible to judge whether FITC-LPS was intra- or extra-sinusoidal and to assess its proximity to KCs. In the composite images (Fig. 2, C–E), VE-cadherin is white, F4/80 is red, DAPI is blue, and FITC is green. The FITC-LPS was almost always found in contact with KCs, although some was free within the sinusoids. We found very little FITC outside sinusoids (i.e., in hepatocytes). We further confirmed that intrasinusoidal FITC-LPS was KC-associated by depleting KCs with clodronate-liposomes prior to injecting FITC-LPS. As shown in Fig. 2D, we found intrasinusoidal FITC (green) in the absence of KCs (red) 24 hours after injection. Although there was green fluorescence within sinusoids at the 7 day time point, very little co-localized with the F4/80-positive cells that had re-populated the sinusoids at that time (Fig. 2E).

The two LPS forms had somewhat different fates after they arrived in the liver. One hour, 4 hrs, and 1 day after injecting FITC-LPS, green fluorescence was found within sinusoids, where it was largely, but not entirely, within or adjacent to KCs (red)(Fig. 2C, Fig. 3A–C). Similar results were found 7 days after injection (not shown). Although the FITC in FITC-LPS-HDL complexes was found within sinusoids one hour after injection, there was little apparent association with KCs (Fig. 3D) and FITC was also found overlying extrasinusoidal cells (arrows). At 4 hrs after injection, however, and again at 24 hrs, more of the FITC from the FITC-LPS-HDL complexes co-localized with KCs (Fig. 3E, F). Free FITC and FITC-BSA, used as controls, were not detectable in the liver sections 1 hour or 3 days after intravenous injection (not shown).

A semiquantitative estimation of FITC-LPS and FITC-LPS-HDL distribution within the liver is shown in Table 1. One hour after injection, 83% of the FITC from FITC-LPS co-localized with KCs, whereas only 49% of the FITC-LPS-HDL was KC-associated. At 4 hrs after injection, 72% of the FITC from FITC-LPS-HDL co-localized with KCs, compared to 94% of the FITC from free FITC-LPS.

We identified neutrophils in liver sections by using an antibody to CD11b that does not bind to KCs in liver sections (not shown). At 1 hr and 1 day after FITC-LPS injection, increased numbers of neutrophils were found in the liver, but only rarely was the FITC label found with these cells. The absence of FITC-LPS in neutrophils was not unexpected, since in previous studies we found that depleting neutrophils by prior treatment with an anti-Gr-1

antibody did not reduce the recovery of [3H/14C]LPS from the liver 15 hrs after i.v. injection (88.4 ± 2.4% was recovered from control mice versus 87.9±4.17% from neutrophil-depleted mice)(6). These results suggest strongly that neutrophils do not play a significant role in liver uptake of free LPS.

Deacylation of LPS and LPS-HDL *in vivo*

Hepatic uptake of LPS-HDL can be blocked by excess HDL (23), suggesting strongly that the complexes are taken up via mechanisms that normally clear HDL. Whereas macrophages express receptors that can bind HDL (SR-BI), HDL can also be taken up by hepatocytes, bypassing Kupffer cells. It was of interest to know whether the LPS in these complexes undergoes deacylation in the liver, since the deacylating enzyme, AOAH, is principally produced by Kupffer cells and not by hepatocytes (6). Unexpectedly, we found that “free” LPS and the LPS in LPS-HDL complexes underwent deacylation at approximately the same fractional rate (Fig. 4A); the amount of deacylated LPS in the liver at 4 and 22 hrs was greater for LPS than for LPS-HDL (Fig. 4B), in keeping with the greater amount of free LPS that had been cleared by the liver at each time point. Kupffer cell depletion decreased the uptake of free LPS by 65% without altering the uptake of LPS-HDL (Fig. 5A); the deacylation of both free and lipoprotein-bound LPS, measured 4 hrs after injection, decreased by approximately 20% (Fig. 5B). Clodronate treatment did not significantly diminish AOAH activity in plasma (n = 6 mice/group, data not shown), suggesting an explanation for the relatively minor impact of Kupffer cell depletion on LPS-deacylating activity in the liver.

DISCUSSION

How the liver disposes of bacterial endotoxin has intrigued investigators for many years. The liver’s ability to take up and inactivate LPS is thought to influence phenomena as diverse as energy intake (40), carbohydrate and lipid metabolism (“metabolic endotoxemia” (41), alcoholic liver disease (42;43), and immune responses in HIV-infected individuals (44). Recent studies have also highlighted the important role that plasma lipoproteins can play in LPS clearance from the blood, and differences have been found in the ability of certain lipoproteins to transport and deliver LPS to hepatic cells. An apoErich emulsion reduced LPS uptake by the liver and increased delivery to hepatocytes (45), for example, and chylomicrons, which may promote intestinal absorption of LPS (46), increased hepatic uptake while shunting LPS away from Kupffer cells (25).

The present experiments were performed after we had observed that (1) almost all of the LPS that is taken up by the liver undergoes enzymatic deacylation (thus, inactivation) within 2 to 3 days (6), and (2) the deacylating enzyme, acyloxyacyl hydrolase (AOAH), is produced by KCs and hepatic dendritic cells (6). Since others have reported that lipoprotein-bound LPS interacts directly with hepatocytes, which do not produce AOAH (6), we wanted to know whether the LPS in LPS-HDL complexes also undergoes deacylation in the liver. We found that LPS and LPS-HDL were deacylated at approximately the same rate, despite striking differences in both the rate of LPS uptake by the liver and its intrahepatic location (much less of the LPS in LPS-HDL complexes was found near or in KCs during the first 4

hours after injection, Fig. 3). This result suggests that plasma AOAH, in addition to that released by KCs, deacylates LPS within sinusoidal blood or, possibly, within SECs, stellate cells, or hepatocytes that have taken up both AOAH and LPS (or LPS-HDL) from the blood.

Some previous studies of LPS clearance used very large and undoubtedly non-physiological LPS inocula, whereas in others the LPS was injected directly into the portal vein, thus achieving very high intrasinusoidal LPS concentrations and minimizing mixing of LPS with blood constituents. We sought to avoid these problems by injecting small doses via the lateral tail vein. On the other hand, our conclusions regarding the localization of LPS in the liver may be limited by the possibility that detection of the FITC chromophore, even after Qdot amplification, will decrease as FITC-LPS aggregates disperse or FITC-LPS-HDL complexes break up *in vivo*. The apparent increase in sinusoidal and KC-associated FITC that occurred between 1 and 4 hours after injection of FITC-LPS-HDL (Fig. 3, D and E, and Table 1) thus might reflect the loss of extrasinusoidal FITC signal due to dispersion of FITC-LPS within hepatocytes or other cells. It is also possible that the FITC-LPS linkage was disrupted *in vivo*; the conjugate was stable in ethanol, however, and neither FITC-glycine nor FITC-BSA was detectable in the liver following i.v. injection.

We conclude that the LPS in LPS-HDL complexes can remain sinusoidal for hours, become at least partially KC-associated, and undergo deacylation by AOAH. Since AOAH-mediated deacylation inactivates LPS, further studies are needed to test the hypothesis that AOAH-mediated LPS inactivation ameliorates both metabolic and infectious diseases of the liver.

Acknowledgments

We thank Dr. Mingfang Lu for advice and helpful discussions and Patricia Thompson for making LPS-HDL complexes. This work was supported by National Institutes of Health grants AI-018188 and AI-045896 from the National Institute of Allergy and Infectious Diseases, the Jan and Henri Bromberg Chair in Internal Medicine (UT-Southwestern) and, in part, by the Intramural Research Program of NIAID.

Abbreviations

AOAH	acyloxyacylhydrolase
DAPI	4’,6-diamidino-2-phenylindole
FITC	fluorescein isothiocyanate
HDL	high-density lipoprotein
KC	Kupffer cells
LDL	low-density lipoprotein
SEC	sinusoidal endothelial cells
SR-A	macrophage scavenger receptor A
SR-BI	scavenger receptor BI
Tlr4	Toll-like receptor 4

References

1. Mathison JC, Ulevitch RJ. The clearance, tissue distribution, and cellular localization of intravenously injected lipopolysaccharide in rabbits. J Immunol. 1979; 123:2133–2143. [PubMed: 489976]
2. Freudenberg MA, Freudenberg N, Galanos C. Time course of cellular distribution of endotoxin in liver, lungs and kidneys of rats. Br J Exp Pathol. Feb; 1982 63(1):56–65. [PubMed: 7039654]
3. Ge Y, Ezzell RM, Tompkins RG, Warren HS. Cellular distribution of endotoxin after injection of chemically purified lipopolysaccharide differs from that after injection of live bacteria. J Infect Dis. 1994; 169:95–104. [PubMed: 8277203]
4. Ge YM, Ezzell RM, Clark BD, Loiselle PM, Amato SF, Warren HS. Relationship of tissue and cellular interleukin-1 and lipopolysaccharide after endotoxemia and bacteremia. J Infect Dis. 1997; 176:1313–1321. [PubMed: 9359733]
5. Freudenberg N, Piotraschke J, Galanos C, Sorg C, Askaryar FA, Klosa B, et al. The role of macrophages in the uptake of endotoxin by the mouse liver. Virchows Arch B Cell Pathol Incl Mol Pathol. 1992; 61(5):343–349. [PubMed: 1348896]
6. Shao B, Lu M, Katz SC, Varley AW, Hardwick J, Rogers TE, et al. A Host Lipase Detoxifies Bacterial Lipopolysaccharides in the Liver and Spleen. J Biol Chem. May 4.2007 282:13726–13735. [PubMed: 17322564]
7. Shao B, Kitchens RL, Munford RS, Rogers TE, Rockey DC, Varley AW. Prolonged hepatomegaly in mice that cannot inactivate bacterial endotoxin. Hepatology. 2011; 54:1051–1062. [PubMed: 21674560]
8. Nakao A, Taki S, Yasui M, Kimura Y, Nonami T, Harada A, et al. The fate of intravenously injected endotoxin in normal rats and in rats with liver failure. Hepatology. 1994; 19:1251–1256. [PubMed: 8175149]
9. Yasui M, Nakao A, Yuuki T, Harada A, Nonami T, Takagi H. Immunohistochemical detection of endotoxin in endotoxemic rats. Hepatogastroenterology. Sep; 1995 42(5):683–690. [PubMed: 8751235]
10. Takeuchi M, Nakashima Y, Miura Y, Nakagawa K, Uragoh K, Iwanaga S, et al. The localization of lipopolysaccharide in an endotoxemic rat liver and its relation to sinusoidal thrombogenesis: light and electron microscopic studies. Pathol Res Pract. Dec; 1994 190(12):1123–1133. [PubMed: 7792203]
11. Praaning-van, Dalen DP.; Brouwer, A.; Knook, DL. Clearance capacity of rat liver Kupffer, endothelial, and parenchymal cells. Gastroenterology. 1981; 81:1036–1044. [PubMed: 7286581]
12. Freudenberg N, Freudenberg MA, Bandara K, Galanos C. Distribution and localization of endotoxin in the reticuloendothelial system (RES) and in the main vessels of the rat during shock. Path Res Pract. 1985; 179:517–527. [PubMed: 4001029]
13. Van Oosten M, Van Amersfoort ES, Van Berkel TJ, Kuiper J. Scavenger receptor-like receptors for the binding of lipopolysaccharide and lipoteichoic acid to liver endothelial and Kupffer cells. J Endotoxin Res. 2001; 7(5):381–384. [PubMed: 11753207]
14. Scott MJ, Billiar TR. beta 2-integrin induced p38MAPK activation is a key mediator in the CD14/TLR4/MD2-dependent uptake of LPS by hepatocytes. J Biol Chem. Aug 13.2008 283:29433–29446. [PubMed: 18701460]
15. Scott MJ, Liu S, Shapiro RA, Vodovotz Y, Billiar TR. Endotoxin uptake in mouse liver is blocked by endotoxin pretreatment through a suppressor of cytokine signaling-1GÇôdependent mechanism. Hepatology. 2009; 49:1695–1708. [PubMed: 19296467]
16. Kamimoto M, Rung-Ruangkijkrai T, Iwanaga T. Uptake ability of hepatic sinusoidal endothelial cells and enhancement by lipopolysaccharide. Biomed Res. Jun; 2005 26(3):99–107. [PubMed: 16011302]
17. Mimura Y, Sakisaka S, Harada M, Sata M, Tanikawa K. Role of hepatocytes in direct clearance of lipopolysaccharide in rats. Gastroenterology. 1995; 109:1969–1976. [PubMed: 7498663]
18. Bikhazi AB, Jurjus AR, Kamal MT, Al Housseini AM, Saab RN, Jaroudi WA, et al. Kinetics of lipopolysaccharide clearance by Kupffer and parenchyma cells in perfused rat liver. Comp Biochem Physiol C Toxicol Pharmacol. Aug.2001 129:339–348. [PubMed: 11489431]

19. Munford RS, Hall CL, Dietschy JM. Binding of Salmonella typhimurium lipopolysaccharides to rat high-density lipoproteins. Infect Immun. 1981; 34:835–843. [PubMed: 7037642]
20. Kitchens RL, Thompson PA, Munford RS, O'Keefe GE. Acute inflammation and infection maintain circulating phspholipid levels and enhance lipopolysaccharide binding to plasma lipoproteins. J Lipid Res. 2003; 44:2339–2348. [PubMed: 12923224]
21. Tobias PS, Ulevitch RJ. Control of lipopolysaccharide-high density lipoprotein binding by acute phase protein(s). J Immunol. 1983; 131:1913–1916. [PubMed: 6311900]
22. Vesy CJ, Kitchens RL, Wolfbauer G, Albers JJ, Munford RS. LPS binding protein and phospholipid transfer protein release lipopolysaccharides from gram negative bacterial membranes. Infect Immun. 1999; 68:2410–2417. [PubMed: 10768924]
23. Munford RS, Andersen JM, Dietschy JM. Sites of tissue binding and uptake in vivo of bacterial lipopolysaccharide-high density lipoprotein complexes: studies in the rat and squirrel monkey. J Clin Invest. 1981; 68:1503–1513. [PubMed: 7033286]
24. Cai L, Ji A, de Beer FC, Tannock LR, Van der Westhuyzen DR. SR-BI protects against endotoxemia in mice through its roles in glucocorticoid production and hepatic clearance. J Clin Invest. Jan; 2008 118(1):364–375. [PubMed: 18064300]
25. Harris HW, Rockey DC, Chau P. Chylomicrons alter the hepatic distribution and cellular response to endotoxin in rats. Hepatology. May.1998 27:1341–1348. [PubMed: 9581689]
26. Cavaillon J-M, Fitting C, Haeffner-Cavaillon N, Kirsch SJ, Warren HS. Cytokine response by monocytes and macrophages to free and lipoprotein-bound lipopolysaccharide. Infect Immun. 1990; 58:2375–2382. [PubMed: 2114366]
27. Flegel WA, Baumstark MW, Weinstock C, Berg A, Northoff H. Prevention of endotoxin-induced monokine release by human low- and high-density lipoproteins and by apolipoprotein A–I. Infect Immun. 1993; 61:5140–5146. [PubMed: 8225591]
28. Vosbeck K, Tobias P, Mueller H, Allen RA, Arfors K-E, Ulevitch RJ, et al. Priming of polymorphonuclear granulocytes by lipopolysaccharides and its complexes with lipopolysaccharide binding protein and high density lipoprotein. J Leukocyte Biol. 1990; 47:97–104. [PubMed: 2154525]
29. Munford R, Lu M, Varley A. Chapter 2: Kill the bacteria...and also their messengers? Adv Immunol. 2009; 103:29–48. [PubMed: 19755182]
30. Lu M, Varley AW, Ohta S, Hardwick J, Munford RS. Host inactivation of bacterial lipopolysaccharide prevents prolonged tolerance following gram-negative bacterial infection. Cell Host Microbe. Sep 11; 2008 4(3):293–302. [PubMed: 18779055]
31. Lu M, Zhang M, Takashima A, Weiss J, Apicella MA, Li XH, et al. Lipopolysaccharide deacylation by an endogenous lipase controls innate antibody responses to Gram-negative bacteria. Nat Immunol. 2005; 6:989–994. [PubMed: 16155573]
32. Koyama I, Matsunaga T, Harada T, Hokari S, Komoda T. Alkaline phosphatases reduce toxicity of lipopolysaccharides in vivo and in vitro through dephosphorylation. Clin Biochem. Sep; 2002 35(6):455–461. [PubMed: 12413606]
33. Poelstra K, Bakker WW, Klok PA, Hardonk MJ, Meijer DKF. A physiologic function for alkaline phosphatase: Endotoxin detoxification. Lab Invest. 1997; 76:319–327. [PubMed: 9121115]
34. Chen K, Malo M, Beasley-Topliffe L, Poelstra K, Millan J, Mostafa G, et al. A Role for Intestinal Alkaline Phosphatase in the Maintenance of Local Gut Immunity. Dig Dis Sci. Apr 1.2011 56:1020–1027. [PubMed: 20844955]
35. Goldberg RF, Austen WG Jr. Zhang X, Munene G, Mostafa G, Biswas S, et al. Intestinal alkaline phosphatase is a gut mucosal defense factor maintained by enteral nutrition. Proceedings of the National Academy of Sciences. Feb.2008 21:0712140105.
36. Galanos C, Luderitz O, Westphal O. A new method for the extraction of R lipopolysaccharides. Eur J Biochem. 1969; 9:245–249. [PubMed: 5804498]
37. Thompson PA, Tobias PS, Viriyakosol S, Kirkland TN, Kitchens RL. Lipopolysaccharide (LPS)-binding Protein inhibits responses to cell-bound LPS. J Biol Chem. Aug 1; 2003 278(31):28367–28371. [PubMed: 12754215]

38. Kitchens RL, Wolfbauer G, Albers JJ, Munford RS. Plasma lipoproteins promote the release of bacterial lipopolysaccharide from the monocyte cell surface. J Biol Chem. 1999; 274:34116–34122. [PubMed: 10567381]

39. Lu M, Zhang M, Kitchens RL, Fosmire S, Takashima A, Munford RS. Stimulus-dependent deacylation of bacterial lipopolysaccharide by dendritic cells. J Exp Med. 2003; 197:1745–1754. [PubMed: 12810692]

40. Amar J, Burcelin R, Ruidavets JB, Cani PD, Fauvel J, Alessi MC, et al. Energy intake is associated with endotoxemia in apparently healthy men. Am J Clin Nutr. May 1.2008 87:1219–1223. [PubMed: 18469242]

41. Cani PD, Bibiloni R, Knauf C, Waget A, Neyrinck AM, Delzenne NM, et al. Changes in gut microbiota control metabolic endotoxemia-induced inflammation in high-fat diet-induced obesity and diabetes in mice. Diabetes. Jun; 2008 57(6):1470–1481. [PubMed: 18305141]

42. Miller AM, Horiguchi N, Jeong WI, Radaeva S, Gao B. Molecular Mechanisms of Alcoholic Liver Disease: Innate Immunity and Cytokines. Alcoholism: Clinical and Experimental Research. 2011; 35:787–793.

43. Szabo G, Bala S. Alcoholic liver disease and the gut-liver axis. World J Gastroenterol. Mar 21; 2010 16(11):1321–1329. [PubMed: 20238398]

44. Brenchley JM, Price DA, Schacker TW, Asher TE, Silvestri G, Rao S, et al. Microbial translocation is a cause of systemic immune activation in chronic HIV infection. Nat Med. Dec; 2006 12(12):1365–1371. [PubMed: 17115046]

45. Rensen PCN, Van Oosten M, Van de Bilt E, Van Eck M, Kuiper J, Van Berkel TJC. Human recombinant apolipoprotein E redirects lipopolysaccharide from Kupffer cells to liver parenchymal cells in rats in vivo. J Clin Invest. 1997; 99:2438–2445. [PubMed: 9153287]

46. Ghoshal S, Witta J, Zhong J, de Villiers W, Eckhardt E. Chylomicrons promote intestinal absorption of lipopolysaccharides. J Lipid Res. Jan 1.2009 50:90–97. [PubMed: 18815435]

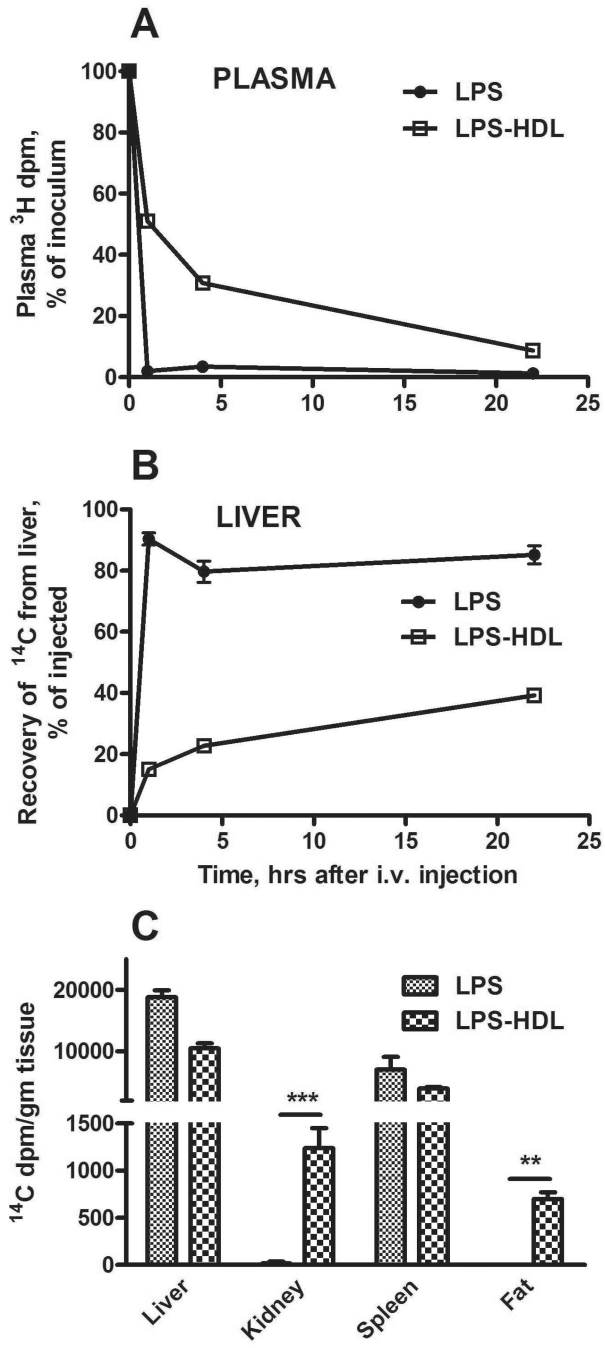

Figure 1. Plasma clearance and tissue uptake of radiolabeled LPS and HDL-LPS

LPS or HDL-LPS, each containing 5 μg [^{3}H/^{14}C]LPS, was injected via the lateral tail vein. **A** and **B** show the time course for disappearance of LPS and LPS-HDL from the plasma (**A**) and their uptake by the liver (**B**). **C** compares the tissue distribution of LPS and LPS-HDL 22 hrs after i.v. injection. n = 3–6 mice/timepoint. Error bars = 1 SEM. Data combined from 3 experiments with similar results. ** $p < 0.01$, *** $p < 0.001$.

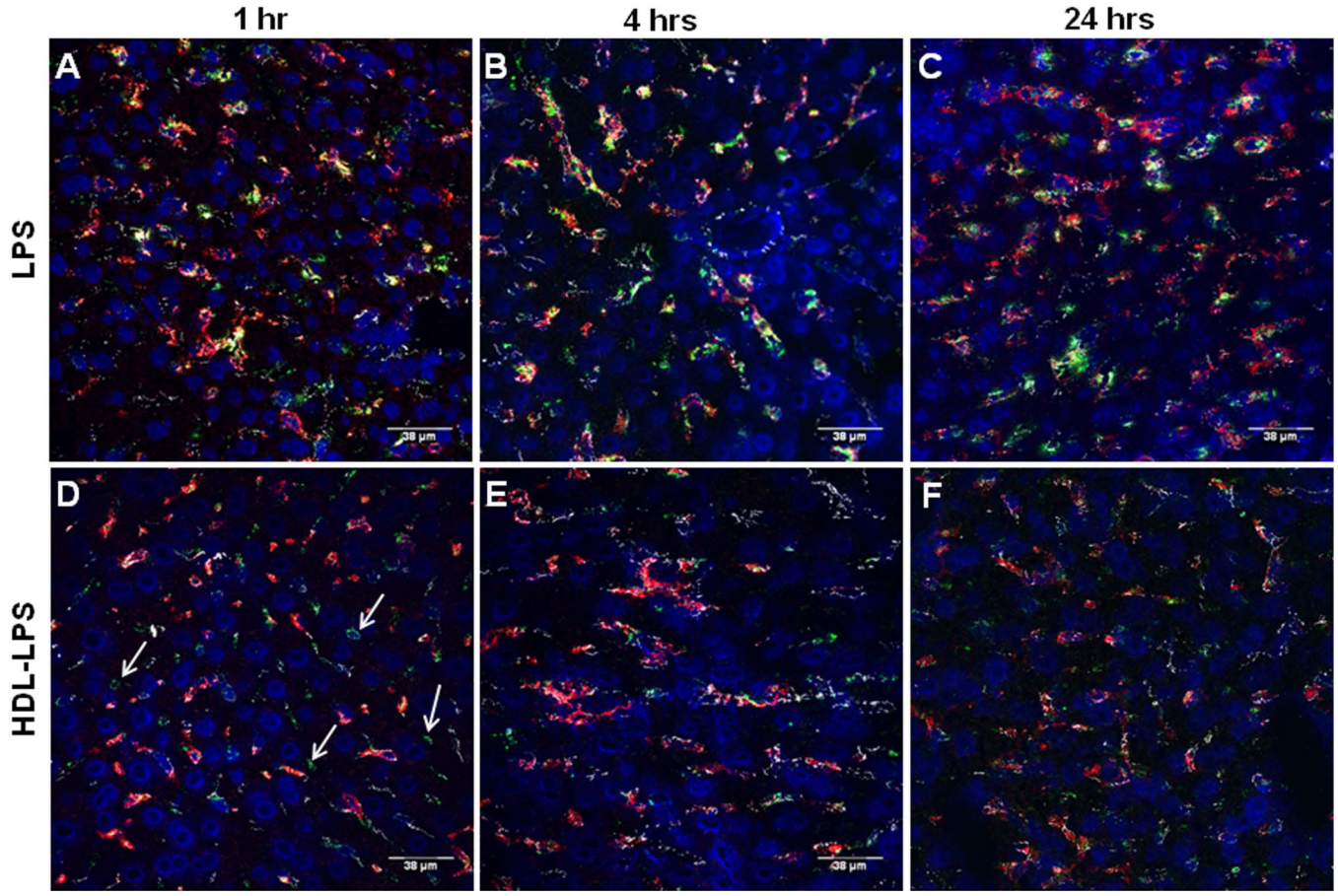

Figure 2. Uptake of FITC-LPS by liver cells

A. Sinusoidal endothelial cell junctions were stained with anti-CD144 (VE-cadherin), which is red in this panel. FITC-LPS is green. Cell nuclei are blue (DAPI). Note that the red label outlines many of the sinusoids. **B**. In the same image, Kupffer cells were stained with anti-F4/80 (red). **C**. shows the merged image, with the VE-cadherin now shown in white. Note that the FITC (green) is almost always found in contact with Kupffer cells (arrowheads), although some is also free within the sinusoids and there is occasional extrasinusoidal FITC as well (arrow). **D–E**. FITC-LPS is shown 1 day (D) and 7 days (E) after FITC-LPS administration to mice that had received clodronate liposomes 48 hours before as described in Methods. FITC-LPS (green), KC (F4/80, red), SEC (VE-cadherin, white), and nuclei (DAPI, blue).

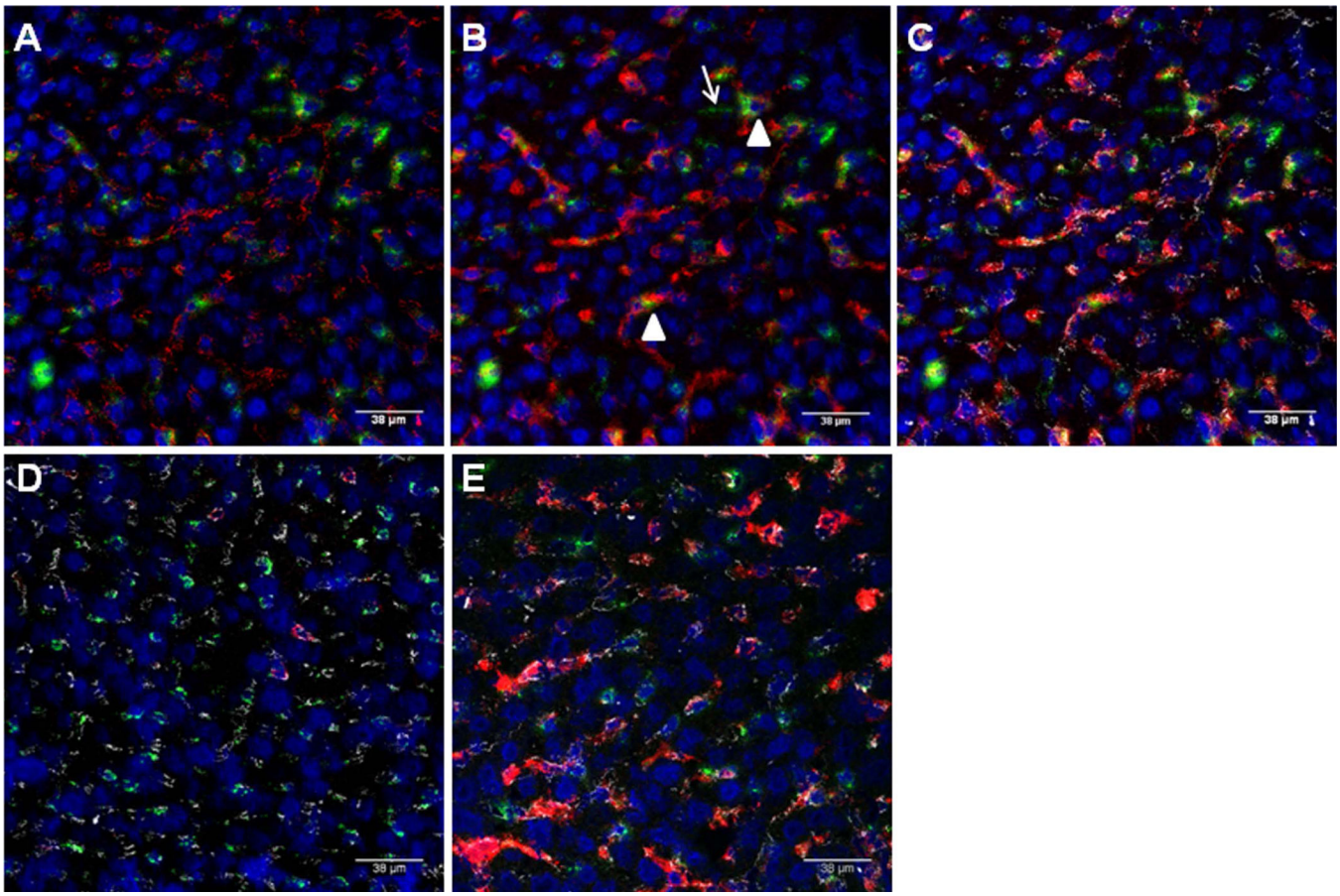

Figure 3. LPS and LPS-HDL uptake by the liver

Each panel shows a merged image with VE-cadherin (white), Kupffer cells (red), FITC-LPS (green), and cell nuclei (blue). **A–C**, FITC-LPS; **D–F**, FITC-LPS-HDL. At 1 hr after injection, most of the FITC-LPS is associated with Kupffer cells (A), whereas most of the FITC-LPS-HDL is within sinusoids but not KC-associated and some may be extrasinusoidal (D, arrows). By 4 and 24 hrs after injection, more of the FITC-LPS-HDL is in close proximity to KCs (E and F), yet the overlap is not so prominent as it is for FITC-LPS and KCs (B and C).

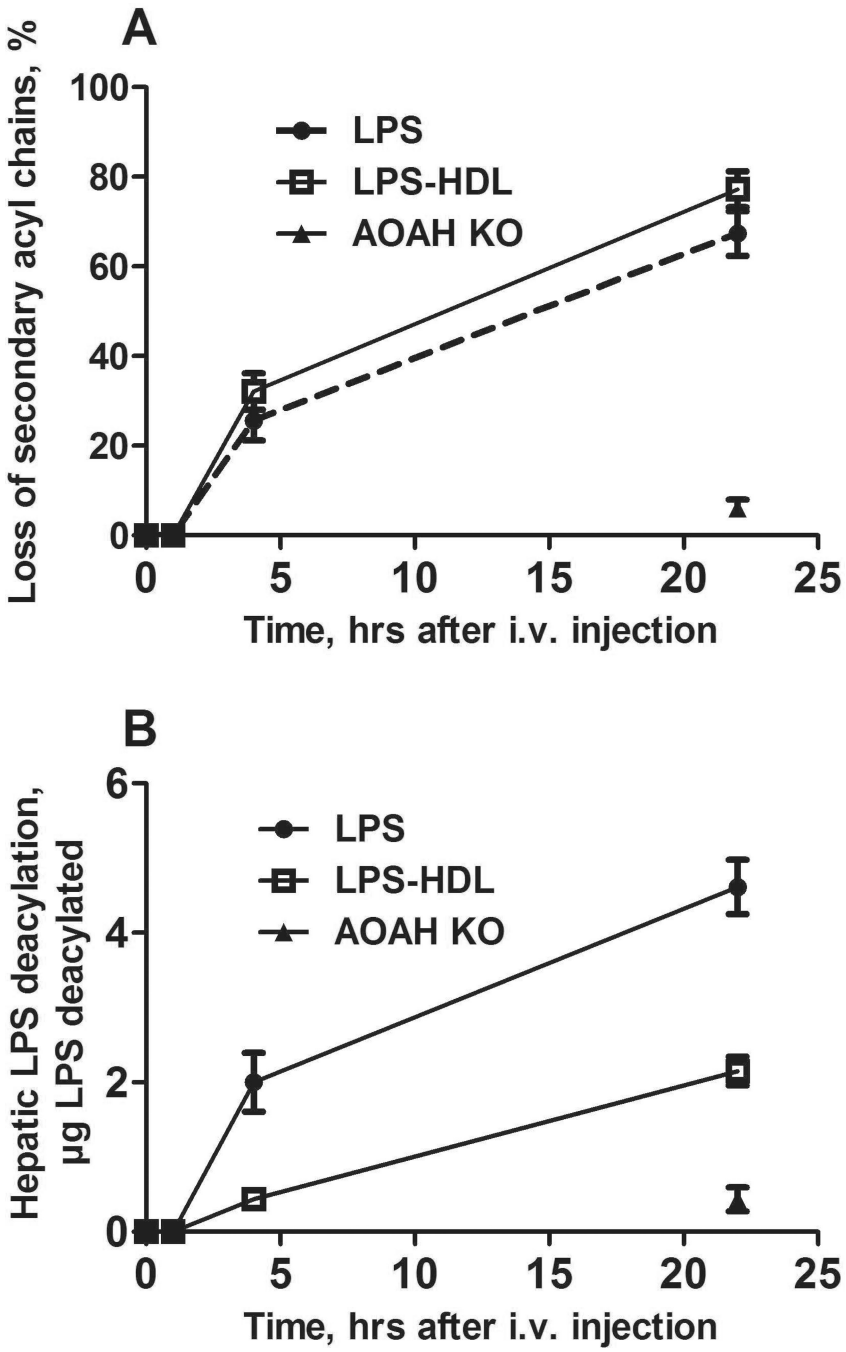

Figure 4. Time course of LPS deacylation in the liver

Five µg [^{3}H/^{14}C]LPS or [^{3}H/^{14}C]LPS-HDL were injected i.v. at time = 0 and the liver was harvested at the indicated times. **A**. Deacylation at each time point is expressed as the loss of secondary acyl chains from LPS. **B**. The amount of LPS deacylated at each time point is shown. The greater amount of LPS deacylated in B is due to the greater uptake of LPS by the liver; the deacylation rate was similar for LPS and LPS-HDL. AOAH-KO mice (closed triangle) lack AOAH (control). n = 3–6 mice/time point for each LPS preparation. Error bars = 1 SEM. Data combined from 4 experiments with consistent results.

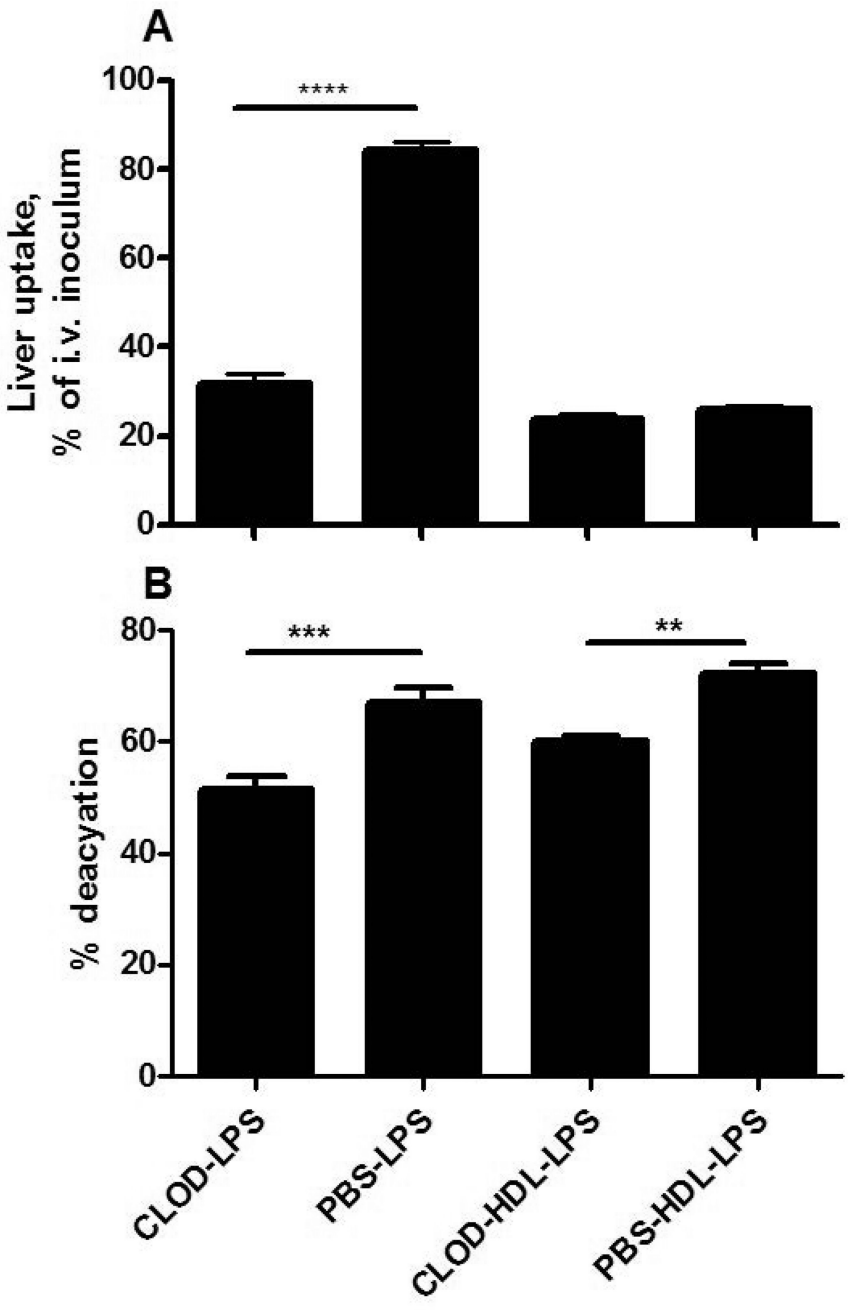

Figure 5. Effect of Kupffer cell depletion on LPS uptake and deacylation in the liver

Hepatic LPS uptake (A) and deacylation (**B**) were measured 4 hours after i.v. injection of LPS or LPS-HDL into mice that had received either PBS-liposomes or clodronate (CLOD) liposomes 2 days earlier. Kupffer cell depletion, documented by staining liver sections for F4/80-positive cells (see Fig. 2D), reduced hepatic uptake of LPS at this early time point but not that of LPS-HDL (**A**). Deacylation of both free LPS and HDL-bound LPS was reduced

by approximately 20%. n = 3 mice/group; The experiment was repeated with similar results. ** $p < 0.01$, *** $p < 0.001$.

Table 1

Analysis of LPS distribution in liver sections.

	F4/80	+	+	−	−
	CD144	+	−	+	−
1 hr	LPS	83±9%	0.4±0.5%	13±9%	4.0±4.7%
	LPS-HDL	49±11%***	0.7±1.8%	35±5%***	15.4±10.2%*
4 hrs	LPS	94±4%	0 ± 0%	5.9±3.9%	0.2±0.3%
	LPS-HDL	72±14%*	0.2±0.8%	25±14%	3.4±4.0%

The percentage of the total FITC-LPS that overlapped or was adjacent to Kupffer cells (F4/80+) or sinusoidal endothelial cells (CD144+) was estimated as described in Methods and shown as mean ± SD (n=6 images) derived from 3 mice/group. Asterisks denote significant difference from the control (LPS) group

* $p<0.05$,

** $p<0.01$,

*** $p<0.001$.